Complexity of viscous dissipation in turbulent thermal convection

Shashwat Bhattacharya, Ambrish Pandey, Abhishek Kumar, and Mahendra K. Verma

Citation: Physics of Fluids **30**, 031702 (2018); doi: 10.1063/1.5022316
View online: https://doi.org/10.1063/1.5022316
View Table of Contents: http://aip.scitation.org/toc/phf/30/3
Published by the American Institute of Physics

Complexity of viscous dissipation in turbulent thermal convection

Shashwat Bhattacharya,[1,a)] Ambrish Pandey,[2,b)] Abhishek Kumar,[3,c)] and Mahendra K. Verma[4,d)]

[1]*Department of Mechanical Engineering, Indian Institute of Technology Kanpur, Kanpur 208016, India*
[2]*Institut für Thermo- und Fluiddynamik, Technische Universität Ilmenau, Ilmenau 98684, Germany*
[3]*Applied Mathematics Research Centre, Coventry University, Coventry CV1 5FB, United Kingdom*
[4]*Department of Physics, Indian Institute of Technology Kanpur, Kanpur 208016, India*

(Received 13 January 2018; accepted 14 March 2018; published online 29 March 2018)

Using direct numerical simulations of turbulent thermal convection for the Rayleigh number between 10^6 and 10^8 and unit Prandtl number, we derive scaling relations for viscous dissipation in the bulk and in the boundary layers. We show that contrary to the general belief, the total viscous dissipation in the bulk is larger, albeit marginally, than that in the boundary layers. The bulk dissipation rate is similar to that in hydrodynamic turbulence with log-normal distribution, but it differs from (U^3/d) by a factor of $\mathrm{Ra}^{-0.18}$. Viscous dissipation in the boundary layers is rarer but more intense with a stretched-exponential distribution. *Published by AIP Publishing.* https://doi.org/10.1063/1.5022316

Physics of hydrodynamic turbulence is quite complex, involving strong nonlinearity and boundary effects. To simplify, researchers have considered hydrodynamic turbulence in a box away from the walls. The turbulence in such a geometry is statistically homogeneous and isotropic. The physics of even such idealised flows remain primarily unsolved, yet their energetics are reasonably well understood. Here, the energy supplied at large length scales cascades to intermediate scales and then to dissipative scales.[1,2] Thus, under steady state, the energy supplied by the external force equals the energy cascade rate, Π_u, and the viscous dissipation rate, ϵ_u. From dimensional analysis, it has been deduced that $\epsilon_u \approx U^3/L$, where U is the large-scale velocity, L is the large length scale, and the prefactor is approximately unity.[3,4]

Thermal convection is a very important problem of science and engineering. Here too researchers have considered an idealised system called *Rayleigh–Bénard convection* (RBC) in which a fluid is confined between two horizontal thermal plates separated by a vertical distance of d; the bottom plate is hotter than the top one.[5–7] The kinematic viscosity (ν) and thermal diffusivity (κ) are treated as constants. Additionally, the density of the fluid is considered to be a constant except for the buoyancy term of the fluid equation. The governing equations of RBC are as follows:

$$\partial_t \mathbf{u} + (\mathbf{u}\cdot\nabla)\mathbf{u} = -\nabla\sigma/\rho_0 + \alpha g\theta\hat{z} + \nu\nabla^2\mathbf{u}, \tag{1}$$

$$\partial_t\theta + (\mathbf{u}\cdot\nabla)\theta = (\Delta/d)u_z + \kappa\nabla^2\theta, \tag{2}$$

$$\nabla\cdot\mathbf{u} = 0, \tag{3}$$

where $\mathbf{u}$ and σ are the velocity and pressure fields, respectively, θ is the temperature fluctuation over the conduction state, ρ_0 and α are, respectively, the mean density and thermal expansion coefficient of the fluid, g is the acceleration due to gravity, and Δ is the temperature difference between the hot and cold plates. RBC is specified by two nondimensional parameters—Rayleigh number $\mathrm{Ra} = (\alpha g\Delta d^3)/(\nu\kappa)$, which is a measure of buoyancy, and the Prandtl number $\mathrm{Pr} = \nu/\kappa$ (see the supplementary material).

For thermal convection, walls and their associated boundary layers play an important role; hence, turbulence in thermal convection is more complex than hydrodynamic turbulence. In this letter, we focus on the properties of the viscous dissipation in RBC. Verzicco and Camussi[8] and Zhang, Zhou, and Sun[9] computed the viscous dissipation rates in the bulk and in the boundary layers in RBC and found them to be of the same order. Here, we perform a detailed analysis of these quantities and their probability distributions, both numerically and phenomenologically. We will show that the walls of thermally driven turbulence introduce interesting and generic features in the viscous dissipation.

Shraiman and Siggia[10] derived an interesting exact relation that relates the viscous dissipation rate, ϵ_u, to the heat flux,

$$\epsilon_u = \langle\epsilon_u(\mathbf{r})\rangle = \left\langle \frac{\nu}{2}\left(\frac{\partial u_i}{\partial x_j} + \frac{\partial u_j}{\partial x_i}\right)^2 \right\rangle = \frac{\nu^3}{d^4}\frac{(\mathrm{Nu}\text{-}1)\mathrm{Ra}}{\mathrm{Pr}^2} = \frac{U^3}{d}\frac{(\mathrm{Nu}\text{-}1)\mathrm{Ra}}{\mathrm{Re}^3\,\mathrm{Pr}^2}, \tag{4}$$

where $\langle\cdot\rangle$ denotes the volume average over the entire domain and u_i with $i = (x, y, z)$ is the ith the component of the velocity field. The Nusselt number, Nu, is the ratio of the total heat flux and the conductive heat flux, and $\mathrm{Re} = UL/\nu$ is the Reynolds number. When the boundary layer is either absent (as in a periodic box) or weak (as in the ultimate regime proposed by Kraichnan[11]), $\mathrm{Nu} \sim (\mathrm{RaPr})^{1/2}$ and $\mathrm{Re} \sim (\mathrm{Ra/Pr})^{1/2}$ (see Refs. 7 and 12–14). Substitution of these relations into Eq. (4) yields $\epsilon_u \sim U^3/d$, similar to hydrodynamic turbulence. In this letter, we focus on $\mathrm{Pr} \sim 1$ and hence we ignore the Prandtl number dependence.

The scaling however is different for realistic RBC for which boundary layers near the plates play an important role.

a)Electronic mail: shabhatt@iitk.ac.in
b)Electronic mail: ambrish.pandey@tu-ilmenau.de
c)Electronic mail: abhishek.kir@gmail.com
d)Electronic mail: mkv@iitk.ac.in

Scaling arguments,[12,15–17] experiments,[5,16,18–21] and numerical simulations[8,22–26] reveal that $\mathrm{Re} \sim \mathrm{Ra}^{1/2}$ and $\mathrm{Nu} \sim \mathrm{Ra}^{0.3}$, substitution of which in Eq. (4) yields $\epsilon_u \neq U^3/d$, rather

$$\epsilon_u \sim \frac{U^3}{d}\mathrm{Ra}^{-0.2} \sim \frac{\nu^3}{d^4}\mathrm{Ra}^{1.3}, \tag{5}$$

because $U \sim \mathrm{Re} \sim \mathrm{Ra}^{1/2}$. This is due to the relative suppression of the nonlinear interactions in RBC, as Pandey *et al.*,[25] Pandey and Verma,[26] and Verma, Kumar, and Pandey[7] showed that in RBC, the ratio of the nonlinear term and viscous term scales as $(UL/\nu)\mathrm{Ra}^{-0.15}$. The aforementioned suppression of nonlinear interactions leads to weaker energy cascade $\Pi(k)$ and hence lower viscous dissipation than the corresponding hydrodynamic turbulence.

In RBC, the viscous dissipation rates in the bulk and in the boundary layers are very different. In the following discussion, using scaling arguments and the exact relation given by Eq. (4), we will quantify the total viscous dissipation rates in the bulk and boundary layers, $\tilde{D}_{u,\mathrm{bulk}}$ and $\tilde{D}_{u,\mathrm{BL}}$, as well as the corresponding average viscous dissipation rates, $\epsilon_{u,\mathrm{bulk}}$ and $\epsilon_{u,\mathrm{BL}}$, which are obtained by dividing the total dissipation rates by their respective volumes.

Grossmann and Lohse's model[12,13] assumes that $\epsilon_{u,\mathrm{bulk}} \sim U^3/d \sim \mathrm{Ra}^{3/2}$. We find that the average viscous dissipation in the bulk scales similar to the viscous dissipation rate in the entire volume, i.e.,

$$\epsilon_{u,\mathrm{bulk}} \sim \frac{U^3}{d}\mathrm{Ra}^{-0.18}. \tag{6}$$

Since the fluid flow in the boundary layers is laminar, we expect $\epsilon_{u,\mathrm{BL}} \sim \nu U^2/\delta_u^2$, where δ_u is the thickness of the viscous boundary layer. Hence, the ratio of the two dissipation rates is

$$\begin{aligned}\frac{\epsilon_{u,\mathrm{BL}}}{\epsilon_{u,\mathrm{bulk}}} &\sim \mathrm{Ra}^{0.18}\left(\frac{\nu U^2}{\delta_u^2}\right)/\left(\frac{U^3}{d}\right)\\ &\sim \frac{1}{\mathrm{Re}}\left(\frac{d}{\delta_u}\right)^2\mathrm{Ra}^{0.18} \sim \left(\frac{d}{\delta_u}\right)^2\mathrm{Ra}^{-0.32}.\end{aligned} \tag{7}$$

Note, however, that the volume of the boundary layers is much less than that of the bulk. For simplicity, we assume that the fluid is contained in a cube of dimension d, then the ratio of the volumes of the boundary layer and bulk is

$$\frac{V_{\mathrm{BL}}}{V_{\mathrm{bulk}}} \sim \frac{\delta_u d^2}{(d-\delta_u)^3} \sim \frac{\delta_u}{d} \tag{8}$$

because $\delta_u \ll d$ for $\mathrm{Pr} \sim 1$. Using the above relations, we can deduce the scaling of the ratio of the total viscous dissipation rates in the boundary layer and in the bulk as

$$\frac{\tilde{D}_{u,\mathrm{BL}}}{\tilde{D}_{u,\mathrm{bulk}}} \sim \frac{\epsilon_{u,\mathrm{BL}}}{\epsilon_{u,\mathrm{bulk}}} \times \frac{V_{\mathrm{BL}}}{V_{\mathrm{bulk}}} \sim \frac{d}{\delta_u}\mathrm{Ra}^{-0.32}. \tag{9}$$

According to the Prandtl–Blassius theory,[27]

$$\frac{\delta_u}{d} \sim \mathrm{Re}^{-1/2} \sim \mathrm{Ra}^{-1/4} \tag{10}$$

which yields $\tilde{D}_{u,\mathrm{BL}}/\tilde{D}_{u,\mathrm{bulk}} \sim \mathrm{Ra}^{-0.07}$. Thus, in RBC, the total viscous dissipation in the boundary layer and bulk is comparable to each other. For very large Ra, the bulk dissipation outweighs the dissipation in the boundary layer. This is contrary to the general belief that the viscous dissipation occurs primarily in the plumes of the boundary layers.

In this letter, using numerical simulations we show that δ_u/d differs slightly from Eq. (10) and

$$\frac{\delta_u}{d} \sim \mathrm{Re}^{-0.44} \sim (\mathrm{Ra}^{1/2})^{-0.44} \sim \mathrm{Ra}^{-0.22}, \tag{11}$$

using which we find

$$\frac{\tilde{D}_{u,\mathrm{BL}}}{\tilde{D}_{u,\mathrm{bulk}}} \sim \mathrm{Ra}^{-0.10}. \tag{12}$$

Thus,

$$\epsilon_{u,\mathrm{BL}} \sim \frac{\nu U^2}{\delta_u^2} \sim \frac{\nu^3}{d^4}\mathrm{Ra}^{1.44}, \tag{13}$$

$$\tilde{D}_{u,\mathrm{BL}} \sim \epsilon_{u,\mathrm{BL}}\,\delta_u d^2 \sim \frac{\nu^3}{d}\mathrm{Ra}^{1.22}, \tag{14}$$

$$\tilde{D}_{u,\mathrm{bulk}} \sim \epsilon_{u,\mathrm{bulk}}\,d^3 \sim \frac{\nu^3}{d}\mathrm{Ra}^{1.32}. \tag{15}$$

Interestingly, $\tilde{D}_{u,\mathrm{BL}} \sim d^2\nu U^2/\delta_u \sim (\nu^3/d)\mathrm{Ra}^{5/4}$, as assumed in Grossmann and Lohse's model.[12,13]

We perform direct numerical simulations of RBC and verify the aforementioned scaling. The simulations were performed using a finite volume code OpenFOAM[28] for $\mathrm{Pr} = 1$ and Ra between 10^6 and 10^8 in a three-dimensional cube of unit dimension. We impose no-slip boundary condition at all the walls, isothermal condition at the top and bottom walls, and adiabatic condition at the sidewalls (see the supplementary material). A second-order Crank-Nicolson scheme is used for time-stepping. The values of ν and κ used in the simulations are shown in Table I, while keeping the temperature difference between the horizontal plates $\Delta = 1$ for all the runs.

We employ 256^3 non-uniform grid points and solve the governing equations of RBC. The grid is finer near the walls so as to adequately resolve the boundary layer. We ensure that minimum 4 grid points are in the boundary layer, thereby satisfying the criterion set by Grötzbach.[29] The ratio of the Kolmogorov length scale η to the average mesh width Δx_{avg} remains greater than unity for each simulation run implying that the smallest length scales are being adequately resolved in our simulations. We observe that the Nusselt numbers computed numerically using $\langle u_z\theta\rangle$ match quite closely with those computed using ϵ_u and Eq. (4). See Table I for the comparison of these two Nusselt numbers. Also, to validate our code, we compute Nu for $\mathrm{Pr} = 6.8$ fluid and verify that it matches quite well with the experimental value of Nu.[30] We further remark that our simulations capture the large-scale quantities—volume-averaged viscous dissipation and Nusselt number—quite well; such quantities are not affected significantly by discretization errors at very small scales. Note that spectral method is more accurate but more complex than a finite volume method; yet a sufficiently resolved finite volume code is quite appropriate for studying large-scale quantities.

First we compute the thickness of the boundary layer, δ_u, for all our runs. For the same, we compute the root mean square horizontal velocity in each horizontal plane and estimate δ_u as the vertical height of the intersection of the tangent to the

TABLE I. Details of our direct numerical simulations performed in a unit box for Pr = 1: the Rayleigh Number (Ra), the kinematic viscosity (ν), the Reynolds Number (Re), the ratio of the Kolmogorov length scale (η) to the average mesh width Δx_{avg}, the Nusselt Number (Nu), the Nusselt number deduced from ϵ_u using Eq. (4) (Nu_S), the number of mesh points in the viscous boundary layer (N_{BL}), the volume fraction of the boundary layer region (V_{BL}/V), and the ratio $\tilde{D}_{u,\text{BL}}/\tilde{D}_{u,\text{bulk}}$.

Ra	ν (=κ)	Re	$\eta/\Delta x_{\text{avg}}$	Nu	Nu_S	N_{BL}	V_{BL}/V	$\tilde{D}_{u,\text{BL}}/\tilde{D}_{u,\text{bulk}}$
1×10^6	0.001	150	4.92	8.40	8.34	10	0.14	0.81
2×10^6	0.000 707 1	212	3.89	10.1	10.3	8	0.12	0.67
5×10^6	0.000 447 2	342	2.87	13.3	13.5	7	0.099	0.65
1×10^7	0.000 32	460	2.32	16.0	15.9	6	0.086	0.63
2×10^7	0.000 223 6	654	1.84	20.0	20.0	5	0.074	0.61
5×10^7	0.000 141 4	1080	1.36	25.5	26.0	4	0.062	0.57
1×10^8	0.000 1	1540	1.09	32.8	32.0	4	0.054	0.56

profile at its local maximum with the slope of the profile at the plates.[23,31,32] Similar computations are performed for the sidewalls. In Fig. 1, we plot δ_u for the horizontal walls and sidewalls. The best fit curves of the data yield

$$\text{at thermal plates:} \quad \delta_u/d = 0.35\text{Ra}^{-0.20}, \tag{16}$$

$$\text{at sidewalls:} \quad \delta_u/d = 0.62\text{Ra}^{-0.23}, \tag{17}$$

$$\text{average:} \quad \delta_u/d = 0.52\text{Ra}^{-0.22}, \tag{18}$$

with the errors in the exponents and prefactors being ≈0.002 and 0.01, respectively. In Fig. 1, we plot the horizontal and sidewall boundary layer thicknesses against Ra. These results, a key ingredient of our scaling arguments [see Eq. (11)], are consistent with earlier studies.[8,23,33] As shown in the inset of Fig. 1, near the wall, the velocity profiles differ slightly from the Prandtl–Blasius profile, a result consistent with those of Scheel, Kim, and White[23] and Shi, Emran, and Schumacher;[32] such deviations are attributed to the perpetual emission of plumes from the thermal boundary layers.

We compute the ratio V_{BL}/V, where V is the total volume, using δ_u and Eq. (8). In Table I, we list this ratio for various Ra's. Clearly, the boundary layer occupies much less volume than the bulk, and the ratio decreases with Ra as $\delta_u/d \propto \text{Ra}^{-0.22}$ [see Eq. (11)].

After this, from the numerical data we compute the total dissipation rates in the bulk and in the boundary layer by computing $\int d\tau \epsilon_u(\mathbf{r})$ over the respective volumes. In Fig. 2(a), we plot these values for various Ra's. Best fit curves for these data sets yield

$$\tilde{D}_{u,\text{bulk}} \approx 0.05\frac{\nu^3}{d}\text{Ra}^{1.33}, \tag{19}$$

$$\tilde{D}_{u,\text{BL}} \approx 0.2\frac{\nu^3}{d}\text{Ra}^{1.22} \tag{20}$$

which are consistent with the scaling arguments presented in Eqs. (14) and (15). The ratio of the above quantities, plotted in Fig. 2(b) and listed in Table I, is

$$\frac{\tilde{D}_{u,\text{BL}}}{\tilde{D}_{u,\text{bulk}}} \approx 4\text{Ra}^{-0.11} \tag{21}$$

which is consistent with the scaling of Eq. (12). Note that the above ratio, listed in Table I, decreases from 0.81 to 0.56 as

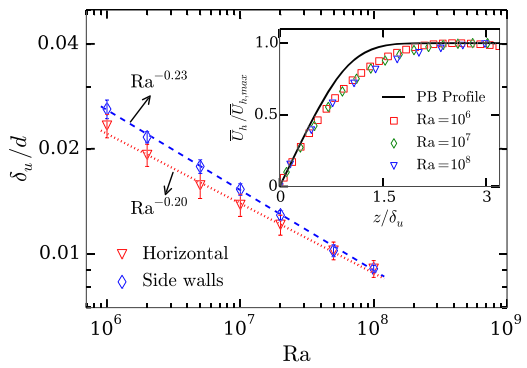

FIG. 1. Plot of normalized boundary layer thickness δ_u/d vs. Ra for horizontal and vertical plates. Best fits are depicted as dashed and dotted lines. Inset shows the comparison of horizontal velocity profiles near the bottom plate with the Prandtl–Blasius profile (solid black line).

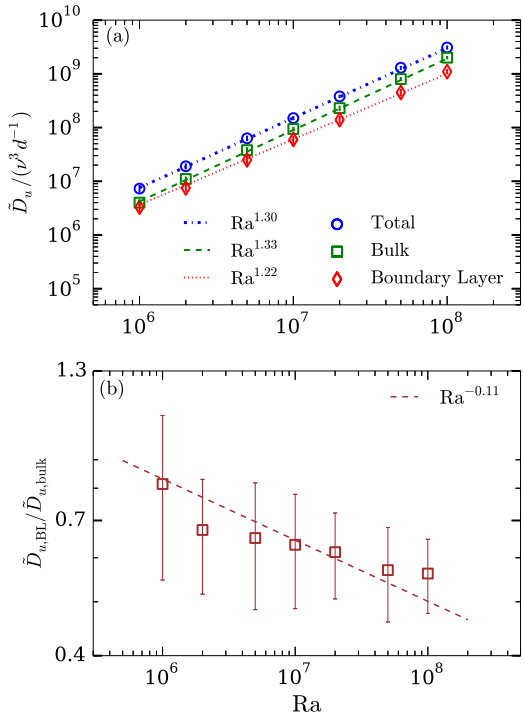

FIG. 2. (a) Plots of the viscous dissipation rates $\tilde{D}_u$—total, bulk, and in the boundary layer—vs. Ra. (b) Plot of the dissipation rate ratio, $\tilde{D}_{u,\text{BL}}/\tilde{D}_{u,\text{bulk}}$, vs. Ra that varies as $\text{Ra}^{-0.11}$.

Ra is increased from 10^6 to 10^8. Thus, bulk dissipation dominates the dissipation in the boundary layer, which is contrary to the belief that viscous dissipation primarily takes place in the boundary layer. It is, however, important to keep in mind that the scaling arguments take inputs from numerical simulations, such as Eq. (18) and Nusselt number scaling.

Thus, both scaling arguments and numerical simulations show that the bulk dissipation is weaker than that in hydrodynamic turbulence, for which $\tilde{D}_{u,\text{bulk}} \sim U^3/d \sim \text{Ra}^{3/2}$. We also compute the total dissipation rate in volume $V_i = (1/4)^3 V$ located deep inside the bulk and observe similar weak scaling with Ra (see the supplementary material). Furthermore, the viscous dissipation in the bulk dominates that in the boundary layer, albeit marginally. The boundary layer, however, occupies much smaller volume than the bulk. Hence, $\epsilon_u(\mathbf{r})$ in the boundary layer is much more intense than in the bulk, which is illustrated in Fig. 3. Here we show density plots of normalized viscous dissipation rate $\epsilon_u(\mathbf{r})/(\nu^3 d^{-4})$ for three planes—in the bottom and a side boundary layer, and in the bulk.

To quantify the asymmetry of the dissipation rate in the bulk and in the boundary layer, for $\text{Ra} = 10^8$, we compute the probability distribution function (PDF) of local viscous dissipation, $\epsilon_u(\mathbf{r})$, over the full volume, the bulk, and the boundary layer. These PDFs, plotted in Fig. 4, reveal many important features. Note that $\epsilon_u(\mathbf{r}) = d\tilde{D}_u/d\tau$ with $d\tau$ as the local volume. For $\epsilon_u(\mathbf{r})/\epsilon_u < 20$, we observe that $\epsilon_{u,\text{bulk}}(\mathbf{r}) \gg \epsilon_{u,\text{BL}}(\mathbf{r})$, and thus, the average dissipation rate in the bulk is relatively weak. But for $\epsilon_u(\mathbf{r})/\epsilon_u > 20$, the viscous dissipation in the boundary layer dominates the bulk dissipation.

In addition, the PDF of $\epsilon_{u,\text{bulk}}$ is log-normal, similar to Obukhov's predictions[34] for the hydrodynamic turbulence. See Fig. 4(a) for an illustration. This is consistent with the results

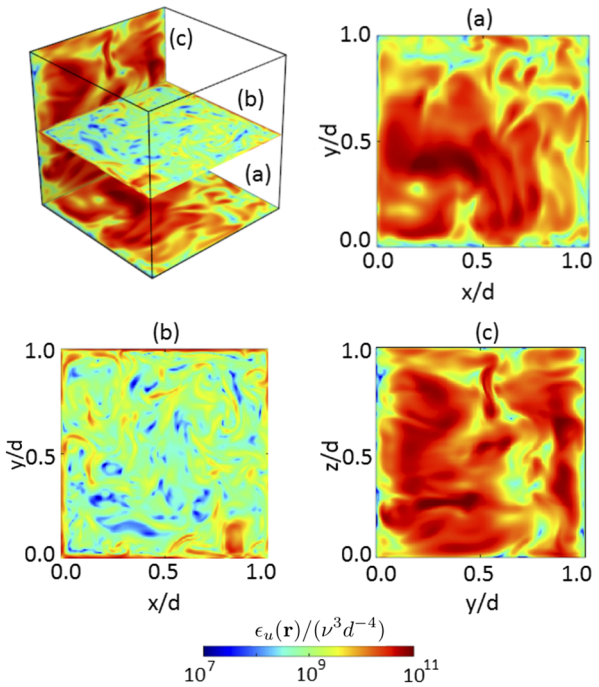

FIG. 3. For $\text{Ra} = 10^8$: Spatial distribution of normalized viscous dissipation rate $\epsilon_u(\mathbf{r})/(\nu^3 d^{-4})$ in planes (a) in the bottom boundary layer at $z = 2\delta_u/3$, (b) in the bulk at $z = 0.5d$, and (c) in one of the sidewall boundary layers at $x = 2\delta_u/3$.

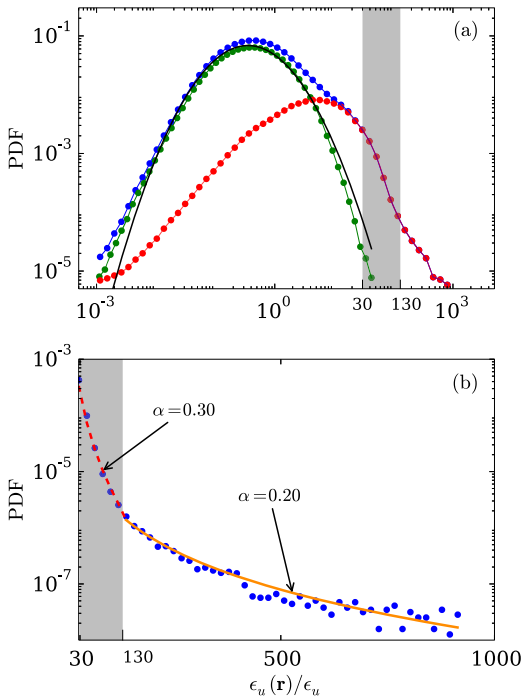

FIG. 4. For $\text{Ra} = 10^8$ and $\text{Pr} = 1$: (a) Probability distribution functions (PDFs) of normalized local dissipation rate ϵ_u in the bulk (green), in the boundary layer (red), and in the entire volume (blue). The bulk ϵ_u has a log-normal distribution (solid black line) with $\sigma = 1.2$ and $\mu = 0.4$. (b) Semilog plot of the PDF of ϵ_u indicates a strong tail for $\epsilon_{u,\text{BL}}$ that fits well with a stretched exponential curve with $\alpha = 0.30$ (dashed red line) in the shaded region and with $\alpha = 0.20$ (solid orange line) outside the region. The shaded region is also shown in (a) for comparison.

of Kumar, Chatterjee, and Verma[35] and Verma, Kumar, and Pandey,[7] who showed similarities between turbulence in RBC and in hydrodynamics. The PDF of $\epsilon_{u,\text{BL}}$, however, is given by a stretched exponential—$P(\epsilon_u) \sim \beta \exp(-m\epsilon_u^{*\alpha})/\sqrt{\epsilon_u^*}$ with $\alpha \approx 0.20$ for $\epsilon_u(\mathbf{r})/\epsilon_u > 130$ and $\alpha \approx 0.30$ for $30 < \epsilon_u(\mathbf{r})/\epsilon_u < 130$ [see Fig. 4(b)]. Here ϵ_u^* correspond to those values of ϵ_u, which are larger than the abscissa of the most probable value. This result indicates that the extreme dissipation takes place inside the boundary layer. We also carry out the PDF analysis of $\epsilon_{u,\text{BL}}$ for $\text{Ra} = 10^6$ and 10^7 and observe similar findings (see the supplementary material). Our detailed work is consistent with earlier results.[8,9] Emran and Schumacher[36] reported similar PDF for the thermal dissipation rate.

We remark that by conducting a similar analysis for $\text{Pr} = 6.8$ and moderate Rayleigh numbers, we observe nearly identical scaling behaviour and distribution of the viscous dissipation rate (see the supplementary material). Thus, it can be inferred that our findings are robust.

A combination of scaling and PDF results reveals that the local viscous dissipation in the bulk, $\epsilon_{u,\text{bulk}}(\mathbf{r})$, is weak, but they add up to a significant sum due to a larger volume. On the contrary, the boundary layer exhibits extreme dissipation in a smaller volume. Interestingly, the total dissipation rate in the bulk and in the boundary layers is comparable, with the bulk dominating the boundary layer marginally.

Our findings clearly contrast the homogeneous-isotropic hydrodynamic turbulence and thermally driven turbulence. The dissipation in thermal convection has two components—$\epsilon_{u,\text{bulk}}$, similar to hydrodynamic turbulence, but distinctly

weaker by a factor of $Ra^{-0.18}$, and $\epsilon_{u,BL}$, which is unique to the flows with walls. We believe that a similar approach could be employed to analyse the thermal dissipation rate and heat transport.

See supplementary material for a similar analysis of viscous dissipation for a larger Prandtl number Pr = 6.8 and the Rayleigh number dependence of the probability distribution function.

We thank S. Fauve, R. Lakkaraju, M. Anas, and R. Samuel for useful discussions. Our numerical simulations were performed on Shaheen II at KAUST Supercomputing Laboratory, Saudi Arabia, under the Project No. k1052. This work was supported by the research Grant No. PLANEX/PHY/2015239 from Indian Space Research Organisation, India, and by the Department of Science and Technology, India (No. INT/RUS/RSF/P-03) and Russian Science Foundation Russia (No. RSF-16-41-02012) for the Indo-Russian project.

[1] A. N. Kolmogorov, "The local structure of turbulence in incompressible viscous fluid for very large Reynolds numbers," Proc. R. Soc. Lond. A **434**, 9–13 (1991).
[2] A. N. Kolmogorov, "Dissipation of energy in the locally isotropic turbulence," Proc. R. Soc. Lond. A **434**, 15–17 (1991).
[3] W. D. McComb, *The Physics of Fluid Turbulence*, Oxford Engineering Science Series (Clarendon Press, Oxford, 1990).
[4] M. Lesieur, *Turbulence in Fluids* (Springer-Verlag, Dordrecht, 2008).
[5] G. Ahlers, S. Grossmann, and D. Lohse, "Heat transfer and large scale dynamics in turbulent Rayleigh-Bénard convection," Rev. Mod. Phys. **81**, 503–537 (2009).
[6] D. Lohse and K. Q. Xia, "Small-scale properties of turbulent Rayleigh–Bénard convection," Annu. Rev. Fluid Mech. **42**, 335–364 (2010).
[7] M. K. Verma, A. Kumar, and A. Pandey, "Phenomenology of buoyancy-driven turbulence: Recent results," New J. Phys. **19**, 025012 (2017).
[8] R. Verzicco and R. Camussi, "Numerical experiments on strongly turbulent thermal convection in a slender cylindrical cell," J. Fluid Mech. **477**, 19–49 (2003).
[9] Y. Zhang, Q. Zhou, and C. Sun, "Statistics of kinetic and thermal energy dissipation rates in two-dimensional turbulent Rayleigh–Bénard convection," J. Fluid Mech. **814**, 165–184 (2017).
[10] B. I. Shraiman and E. D. Siggia, "Heat transport in high-Rayleigh-number convection," Phys. Rev. A **42**, 3650–3653 (1990).
[11] R. H. Kraichnan, "Turbulent thermal convection at arbitrary Prandtl number," Phys. Fluids **5**, 1374–1389 (1962).
[12] S. Grossmann and D. Lohse, "Scaling in thermal convection: A unifying theory," J. Fluid Mech. **407**, 27–56 (2000).
[13] S. Grossmann and D. Lohse, "Thermal convection for large Prandtl numbers," Phys. Rev. Lett. **86**, 3316–3319 (2001).
[14] M. K. Verma, P. K. Mishra, A. Pandey, and S. Paul, "Scalings of field correlations and heat transport in turbulent convection," Phys. Rev. E **85**, 016310 (2012).
[15] W. V. R. Malkus, "The heat transport and spectrum of thermal turbulence," Proc. R. Soc. A **225**, 196–212 (1954).
[16] B. Castaing, G. Gunaratne, L. P. Kadanoff, A. Libchaber, and F. Heslot, "Scaling of hard thermal turbulence in Rayleigh-Bénard convection," J. Fluid Mech. **204**, 1–30 (1989).
[17] S. Grossmann and D. Lohse, "Prandtl and Rayleigh number dependence of the Reynolds number in turbulent thermal convection," Phys. Rev. E **66**, 016305 (2002).
[18] X. Qiu and P. Tong, "Temperature oscillations in turbulent Rayleigh-Bénard convection," Phys. Rev. E **66**, 026308 (2002).
[19] E. Brown, D. Funfschilling, and G. Ahlers, "Anomalous Reynolds-number scaling in turbulent Rayleigh–Bénard convection," J. Stat. Mech.: Theory Exp. **2007**, P10005.
[20] D. Funfschilling, E. Brown, A. Nikolaenko, and G. Ahlers, "Heat transport by turbulent Rayleigh–Bénard convection in cylindrical samples with aspect ratio one and larger," J. Fluid Mech. **536**, 145–154 (2005).
[21] A. Nikolaenko, E. Brown, D. Funfschilling, and G. Ahlers, "Heat transport by turbulent Rayleigh-Bénard convection in cylindrical cells with aspect ratio one and less," J. Fluid Mech. **523**, 251–260 (2005).
[22] G. Stringano and R. Verzicco, "Mean flow structure in thermal convection in a cylindrical cell of aspect ratio one half," J. Fluid Mech. **548**, 1–16 (2006).
[23] J. D. Scheel, E. Kim, and K. R. White, "Thermal and viscous boundary layers in turbulent Rayleigh–Bénard convection," J. Fluid Mech. **711**, 281–305 (2012).
[24] J. D. Scheel and J. Schumacher, "Local boundary layer scales in turbulent Rayleigh–Bénard convection," J. Fluid Mech. **758**, 344–373 (2014).
[25] A. Pandey, A. Kumar, A. G. Chatterjee, and M. K. Verma, "Dynamics of large-scale quantities in Rayleigh-Bénard convection," Phys. Rev. E **94**, 053106 (2016).
[26] A. Pandey and M. K. Verma, "Scaling of large-scale quantities in Rayleigh-Bénard convection," Phys. Fluids **28**, 095105 (2016).
[27] H. Schlichting and K. Gersten, *Boundary-Layer Theory*, 8th ed. (Springer-Verlag, Berlin, Heidelberg, 2000).
[28] H. Jasak, A. Jemcov, Z. Tukovic *et al.*, "Openfoam: A C++ library for complex physics simulations," in *International Workshop on Coupled Methods in Numerical Dynamics* (IUC Dubrovnik, Croatia, 2007), Vol. 1000, pp. 1–20.
[29] G. Grötzbach, "Spatial resolution requirements for direct numerical simulation of the Rayleigh-Bénard convection," J. Comput. Phys. **49**, 241–264 (1983).
[30] Q. Zhou, B.-F. Liu, C.-M. Li, and B.-C. Zhong, "Aspect ratio dependence of heat transport by turbulent Rayleigh–Bénard convection in rectangular cells," J. Fluid Mech. **710**, 260–276 (2012).
[31] X. L. Qiu and K. Q. Xia, "Spatial structure of the viscous boundary layer in turbulent convection," Phys. Rev. E **58**, 5816 (1998).
[32] N. Shi, M. S. Emran, and J. Schumacher, "Boundary layer structure in turbulent Rayleigh–Bénard convection," J. Fluid Mech. **706**, 5–33 (2012).
[33] R. Verzicco and R. Camussi, "Prandtl number effects in convective turbulence," J. Fluid Mech. **383**, 55–73 (1999).
[34] A. M. Obukhov, "Some specific features of atmospheric turbulence," J. Geophys. Res. **67**, 3011, https://doi.org/10.1029/jz067i008p03011 (1962).
[35] A. Kumar, A. G. Chatterjee, and M. K. Verma, "Energy spectrum of buoyancy-driven turbulence," Phys. Rev. E **90**, 023016 (2014).
[36] M. S. Emran and J. Schumacher, "Fine-scale statistics of temperature and its derivatives in convective turbulence," J. Fluid Mech. **611**, 13–34 (2008).